EFFECT OF MARINE AEROSOLS ON THE ALTERATION OF SILICATE GLASSES

Teresa Palomar[1,2,3*], Anne Chabas[4], David M. Bastidas[3], Daniel de la Fuente[3], Aurelie Verney-Carron[4]

[1] Higher Education Institution of Glass, Spanish Glass Foundation, The Royal Glass Factory of La Granja, P° Pocillo, 1, 40100 La Granja de San Ildefonso (Segovia), Spain

[2] Research Unit VICARTE "Vidro e Cerâmica para as Artes", Campus de Caparica, FCT-UNL, Quinta da Torre, 2829-516 Caparica, Portugal

[3] Dept. Surface Engineering, Corrosion & Durability, National Centre for Metallurgical Research (CENIM), CSIC. Ave. Gregorio del Amo 8, 28040 Madrid, Spain

[4] Laboratoire Interuniversitaire des Systèmes Atmosphériques (LISA), UMR CNRS 7583, Université Paris-Est et Université Paris Diderot, 61 avenue du Genéral de Gaulle, 94010 Créteil Cedex, France

[*]Corresponding Author, Tel.: + 351 212 948 300E-mail Address: t.palomar@fct.unl.pt (T. Palomar)

ABSTRACT

This work is focused on the effect of marine aerosols on soda-lime, potash-lime and lead silicate glass samples. Two kinds of tests were carried out, the first one under laboratory controlled condition during 36 days to evaluate the alteration of glass surface by NaCl aerosols, and the second one in a marine atmosphere in Cabo Vilano (Galicia, Spain) for up to three months. Both tests showed similar results. NaCl aerosols acted as condensation nuclei in high humidity environments favoring the lixiviation of the alkaline and alkaline-earth ions from the glass surface and the solubilization of atmospheric gases (CO_2, SO_2).

Marine aerosols could also accelerate the corrosion attack inducing the loss of the surface hydrogen bonds and the opening of the network accelerating the corrosion mechanism. Results also confirmed that high humidity favored the alteration of the glass surface and the formation of new crystalline phases. Soda-lime silicate and lead silicate glasses were the most durable ones, whereas potash-lime silicate glass presented a fissured alteration layer due to the hydrolytic attack of the surface. New crystalline phases including chlorides, carbonates and sulfates were detected on the glass surfaces which can be related to marine aerosols, environmental particles and the reaction of the cations lixiviated from the glass with the atmospheric gases.

Keywords: Glass, Degradation, Sodium chloride, Aerosols.

HIGHLIGHTS

- NaCl aerosols induced the formation of a water layer on the glass surface and the network opening
- High humidity during long time favored the alteration of the glass and the formation of new crystals
- The ions lixiviated from the glass reacted with atmospheric gases solubilized in the water layer

1. INTRODUCTION

Stained glass windows are the historical glasses the most affected by atmospheric degradation because they are located as part of the facade of the buildings daily submitted to wet and dry deposition. They are affected by soiling, which concerns the deposit of soot particles and soluble salts over the glass surface. These deposits can be anthropic, biogenic, terrigenous or marine [1], and can generate a loss of transparency and an increase of the roughness and the hygroscopicity of the surface [2].

Stained glass windows also undergo chemical alteration. The water retained by the glass surface can induce the hydrolytic attack of the glass by the breaking of the siloxane bonds (Eq. 1) and the lixiviation of the alkaline ions (Eq. 2). In acid environments, the lixiviation of alkaline-earth ions can also occur accelerating the degradation rate of the glass (Eq. 3) [3-6].

$$\equiv Si\text{-}O\text{-}Si\equiv + H_2O \leftrightarrow 2\ \equiv Si\text{-}OH \quad (1)$$

$$\equiv Si\text{-}O\text{-}M + H_2O \rightarrow \equiv Si\text{-}OH + M^+ + OH^- \quad (2)$$

$$\equiv Si - O - Ca - O - Si \equiv\ + 2\ H_2O \xrightarrow{pH \ll 7} 2\ \equiv Si - OH\ +\ Ca(OH)_2 \quad (3)$$

As consequence of the hydrolytic attack, the altered areas present a high content of silanol groups (Eq. 1-3) which can polymerize between them to form a porous network enriched in SiO_2 (Eq. 1) [7]. The diffusion of environmental water molecules is favored in these areas, and they can react with the bulk glass to form pits or degradation layers [3, 8-11].

Dealkalization produces also the accumulation of OH^- groups in the altered areas (Eq. 2, 3), which can transform the hydrolytic attack into a basic one. This basic

attack accelerates the breaking of the siloxane bonds and the dissolution of the glass structure accelerating the alteration rate, mainly at pH > 9 (Eq. 4) [12, 13].

$$\equiv Si\text{-}O\text{-}Si\equiv + OH^- \rightarrow \equiv Si\text{-}OH + \equiv Si\text{-}O^- \quad (4)$$

Tensions between altered and unaltered areas can generate fissures, cracks and craters [14, 15]. Additionally, the ions leached during the hydrolytic attack can react with atmospheric gases (CO_2, SO_2, NO_x) to form deposits over the surface and inside the cracks (Eq. 5, 6) [16-19]. The most common deposits are carbonates (calcite) and sulfates (gypsum and syngenite) [20-24].

$$Ca(OH)_2 + CO_2 \rightarrow CaCO_3 + H_2O \quad (5)$$

$$CaCO_3 + SO_2 + ½\ O_2 + 2\ H_2O \rightarrow CaSO_4{\cdot}2H_2O + CO_2 \quad (6)$$

Several works have assessed the influence of atmospheric conditions, especially climatic factors and pollution, on the degradation mechanism, either in real environments [2, 25-28] or in climatic chambers [5, 29, 30]. These studies proved that high relative humidity and high concentration of gaseous pollutants accelerate the degradation rate of historical glasses. Moreover, soiling, deposited particles and chemical alteration can provide exogenous elements for secondary phases or change the local condition of water retention and the chemical composition of the water film [18]. The presence of salts increased the glass degradation by extending the time of wetness of the glass surface and forming saline solutions in the case of deliquescent salts [31]. However, the influence of the marine aerosols on atmospheric degradation of glasses is poorly studied. The deposition of saline particles from marine atmospheres is known to accelerate the degradation of historical stone materials [32-34]. In aqueous solution, other studies have demonstrated that the salts from seawater lead to increase the corrosion rate of quartz, silica [35-40] and silicate glasses [41, 42]. The proposed

mechanism points that alkaline cations in aqueous solutions were easily exchanged by protons from the silanol groups. Due to the steric hindrance, these bonds were situated perpendicularly to the surface, favoring the opening of the structure and, consequently, raising the degradation rate [35]. The same mechanism could occur with the deposit of marine aerosols on the glass surface because the alkaline chlorides (NaCl, KCl…) are the major contributors of marine aerosols, but the information about the effect of atmospheric salinity on glass degradation is scarce.

The alteration of glass is also dependent of its chemical composition. Generally, the most vulnerable glasses to the alteration are those with high content of alkali ions, mainly potassium, or low content of stabilizer ions, such as calcium or magnesium [43, 44]. However soda-lime silicate glasses can also be altered by environmental factors [15, 23].

Therefore, the main objective of this work is to assess the influence of NaCl particles, the principal marine aerosols, on the degradation of glasses with three different compositions: soda-lime silicate, potash-lime silicate and lead silicate glasses. Two experiences were developed, in laboratory and in a real environment. The laboratory tests were set up in order to evaluate the alteration of the glass surfaces caused by NaCl aerosols in temperate climates [45]. The laboratory results were compared afterwards with the glass alteration in the marine atmosphere of Cabo Vilano (Galicia, Spain), which is a more complex real environment.

This research will be especially useful to evaluate the conservation of historical stained glass windows located in places near the coast.

2. EXPERIMENTAL

2.1. Glass Samples

Three model glasses were formulated in the laboratory following the composition of the main representative historical glass types (Table 1). Glass NCS was a soda-lime silicate glass, similar to modern conventional window glasses [46]; glass KCS was a potash-lime silicate glass with similar composition to medieval glasses [47, 48]; and glass PS was a lead silicate glass with high content of PbO, similar to crystal glass [49]. The raw materials were melted at 1450 ºC, for the KCS and PS glasses, and 1550 ºC, for the NCS glass, during 3 h and then annealed from 600 ºC to environmental temperature during 6 h.

The obtained model glasses were cut in slices of 10 × 10 × 2 mm and then polished using emery paper and an aqueous suspension of cerium oxide to obtain optical quality. Previous to the experiment, the samples were cleaned with ethanol to remove organic adsorbents or oily species in the surface which could affect the tests.

Table 1. Chemical composition of the glasses used in this study analyzed by semi-quantitative XRF and normalized to 100% (wt. %).

	Chemical composition															
Glass	Na_2O	MgO	Al_2O_3	SiO_2	P_2O_5	SO_3	K_2O	CaO	TiO_2	MnO	Fe_2O_3	ZnO	As_2O_3	Sb_2O_3	BaO	PbO
NCS	15.1	4.7	1.9	71.5	-	0.3	0.3	8.4	-	0.0	0.1	-	-	-	-	-
KCS	0.8	2.9	3.6	46.2	3.3	-	21.9	20.5	0.1	-	-	-	-	-	-	-
PS	8.6	-	0.3	60.9	-	-	5.0	0.1	-	-	-	1.2	0.4	0.9	3.3	15.4

2.2. Laboratory corrosion tests

The laboratory experience was developed to evaluate the alteration of the glass surfaces caused by NaCl aerosols in temperate climates [45]. NaCl was deposited on the glass samples. For that, samples were placed inside the CIME corrosion chamber developed to simulate dry atmospheric deposition on materials [50]. A solution of 100

g/L NaCl was prepared and nebulized into CIME using an AGK 2000 (Palas®) collision-type atomizer equipped with a dryer system. To increase in a realistic manner the production of marine aerosol, 100 g/L NaCl only represents four times the concentration of this salt in seawater and three times its salinity [51, 52].

Samples were then subject to different levels of relative humidity (RH): 100 % RH, 23 % RH, and cycles 23/100 % RH, which represented the day/night cycle, and a constant temperature of 20 °C. Three samples of each glass (NCS1, KCS1, PS1) were placed in a sealed box whose bottom is filled with ultrapure MilliQ water to maintain the RH at 100 %, three other samples (NCS3, KCS3, PS3) in a second box filled with a supersaturated saline solution of CH_3COOK used to fix the RH at 23 % [53, 54]. For cycles, three samples (NCS2, KCS2, PS2) were weathered for 2 days in the CIME chamber at a daily rate: 23 % RH during 8 hours and at 100 % during 16 hours. Then they were placed inside sealed boxes and switched manually following the same rate during the week and at 100 % during the weekends. The experiment was carried out for 36 days.

2.3. Field exposure

A second kind of test consisted in the exposure of samples (10 × 10 × 2 mm) with the same chemical composition in a real marine atmosphere for up to three months in Cabo Vilano wind farm (Galicia, Spain). They were placed in vertical position unsheltered from the rain in a corrosion station located at 280 m to the shore. It was measured 643.51 mg/(m²·day) of chloride during the exposure period [55]; the atmospheric SO_2 content was negligible. Frequent heavy rainfall and high relative humidity levels were recorded at the test site, indicating prolonged times of wetness of the glass surface [56].

2.4. Characterization techniques

Glass samples were characterized by the following techniques: X-ray fluorescence spectroscopy (XRF), optical microscopy (OM), scanning electron microscopy/energy dispersive X-ray spectroscopy (SEM/EDS), measurement of the contact angles, μ-Raman spectroscopy, Fourier transform infrared spectroscopy (FTIR), grazing incidence X-ray diffraction (GIXRD) and rugosimetry.

Semi-quantitative chemical analyses by XRF were carried out by a S8 TIGER wavelength dispersed X-ray spectrometer equipped with a tube of rhodium, LiF crystal analyzer and generator of 4 kW. The chemical composition of the glasses was calculated with a standard-less analysis program (QUANT-EXPRESS™, software) which depended on fundamental parameters. This method related the measured intensities of characteristic radiations with the concentration of each element in the sample [57].

The optical microscope (OM) was a Leica Leitz Laborlux 12POLS used in the reflection mode and equipped with a CCD camera connected to the Histolab-Microvision® image processing system.

SEM observations of the CIME lab corrosion test were undertaken by a tabletop LV-SEM TM3030 Hitachi® that is a low-vacuum SEM equipped with energy dispersive spectrometer Quantax 70 EDS Bruker. SEM observations of the Cabo Vilano exposition were obtained using the secondary electron detector of a Hitachi S-4800 microscope. An accelerating voltage of 15 kV in charge-up reduction mode has been used in both devices.

Contact angle measurements between the glass samples and distilled water were performed using the Easy Drop Standard “Drop Shape Analysis System” Kruss DSA

100 measurement apparatus under ambient laboratory conditions with the aim of evaluating the wettability of the original glass samples. The contact angle of each glass was measured at least three times, and the average value and standard deviation were calculated.

The μ-Raman spectroscopy analyses were performed with a Labram 300 Jobin Yvon spectrometer, equipped with a solid state laser of 50 mW of power operating at 532 nm. The laser beam was focused either with a ×50 magnification Olympus objective lenses. The analyses were the result of 15 accumulations of 20 seconds carried out with a D0.3 filter. Analyses were performed on the surface of the glasses. Spectra were recorded as an extended scan. The attribution of the Raman spectra was made using the RRUFF database project on minerals.

The measurements of Fourier transform infrared spectroscopy (FTIR) were measured by a 4300 Handheld FTIR spectrometer of Agilent Technologies. The measurements were obtained in Attenuated Total Reflection (ATR) mode with a spectral range from 4000 to 650 cm^{-1} and a spectral resolution of 4 cm^{-1}. Each spectrum was the product of 32 internal scans.

GIXRD measurements were collected with a Bruker AXS D8 diffractometer equipped with a cobalt X-ray tube. A Goebel mirror optics was applied to obtain a parallel and monochromatic X-ray beam. A current of 30 mA and a voltage of 40 kV were employed as tube settings. Operational conditions were selected to obtain X-ray diffraction diagrams with sufficient counting statistics. XRD data was collected with a beam incidence angle of 1˚ between 20 and 100˚ with a step size of 0.03˚ and a counting time of 3 s/step.

The microroughness of the surface was measured with an Optic rugosimeter TRACEiT from Innowep GmbH. 3D topographical maps (5 x 5 mm) were carried out with a resolution of 2.5 μm (Z axis) and 2.5 μm (in X/Y axes). To compare the samples, the roughness maps were flattened and the arithmetic average roughness (Ra) was measured with the software Gwyddion version 2.32 [58].

3. RESULTS

3.1. Lab corrosion test

3.1.1. Morphology of deposits and glass surface properties

Aerosols with an approximately diameter of 1.0 ± 0.5 μm [50], were produced and seeded homogeneously on the surface (Fig. 1a). However, after two days at 100 % RH the deposits looked totally different (Figs. 1b, 1c, 1d). In soda-lime silicate glass, the deposits were small square crystals of ~ 10 μm, although it could be observed big crystals up to 50 μm (Fig. 1b). Lead silicate glasses presented a similar behavior (Fig. 1d). Nevertheless, aerosols on potash-lime silicate glasses formed conglomerates of crystals in form of arrowhead in circular organizations (Fig. 1c).

This difference can be related with the hygroscopic behavior of NaCl aerosols in humid environments and the contact angle of the glasses. In environments with a relative humidity above 76 %, which is the deliquescence point of the NaCl, the particles act as condensation nuclei forming drops on the glass surface [59]. The formation and distribution of these drops depended on the contact angle of the glasses (Table 2). NCS and PS glasses presented a similar contact angle (~ 10˚) and this low value was related with the high wettability of the glass surface [60].

In the corrosion test carried out at 100 % RH, the glass surface was covered by a layer of water where the NaCl aerosols were dissolved. When the samples were taken out, crystals were homogeneously formed on the surface. In KCS samples, the contact angle was ~ 70˚ (Table 2). In these samples, the wettability was less, and independent water drops covered the glass surface [60]. NaCl aerosols were dissolved in each drop, forming the circular conglomerates of crystals (Fig. 1c).

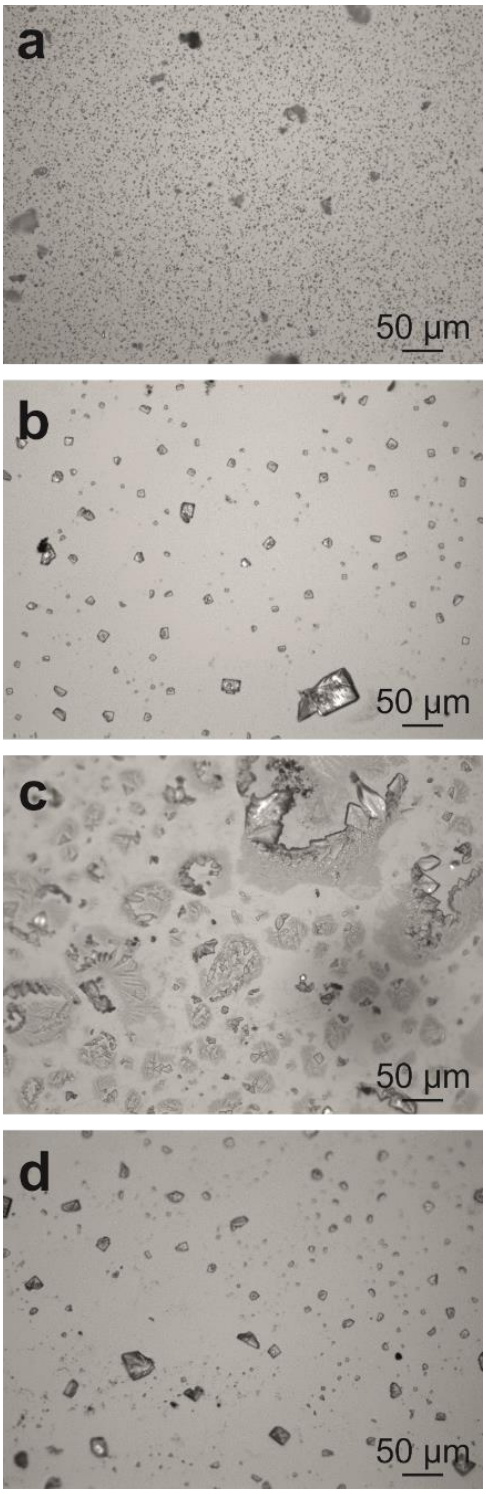

Fig. 1. OM images of a) NCS1 sample after the aerosol deposition, b) NCS1 sample after two days at 100 % RH, c) KCS1 sample after two days at 100 % RH, d) PS1 sample after two days at 100 % RH.

Table 2. Average of contact angle values (in degrees) and standard deviation measured for drops of distilled water on the glass surfaces.

Glass	Contact angle (˚)	Measurement method
NCS	12 ± 6	Circle Fitting
KCS	69 ± 3	Young Laplace
PS	8.9 ± 0.5	Circle Fitting

After 36 days of test, the samples exposed to a high humidity (100 % RH and 100-23 % RH) presented deposits with different morphology. Square and dendritic deposits appeared principally on NCS and PS samples (Figs. 2, 3a, 3c), while KCS samples presented linear and irregular deposits and small fissures on the surface (Figs 2, 3b). In contrast, those samples exposed to 23 % of humidity (NCS3, KCS3 and PS3) presented the same aspect than the original ones because the humidity was not enough to deliquesce the NaCl aerosols (Figs. 1a, 2) [59, 61].

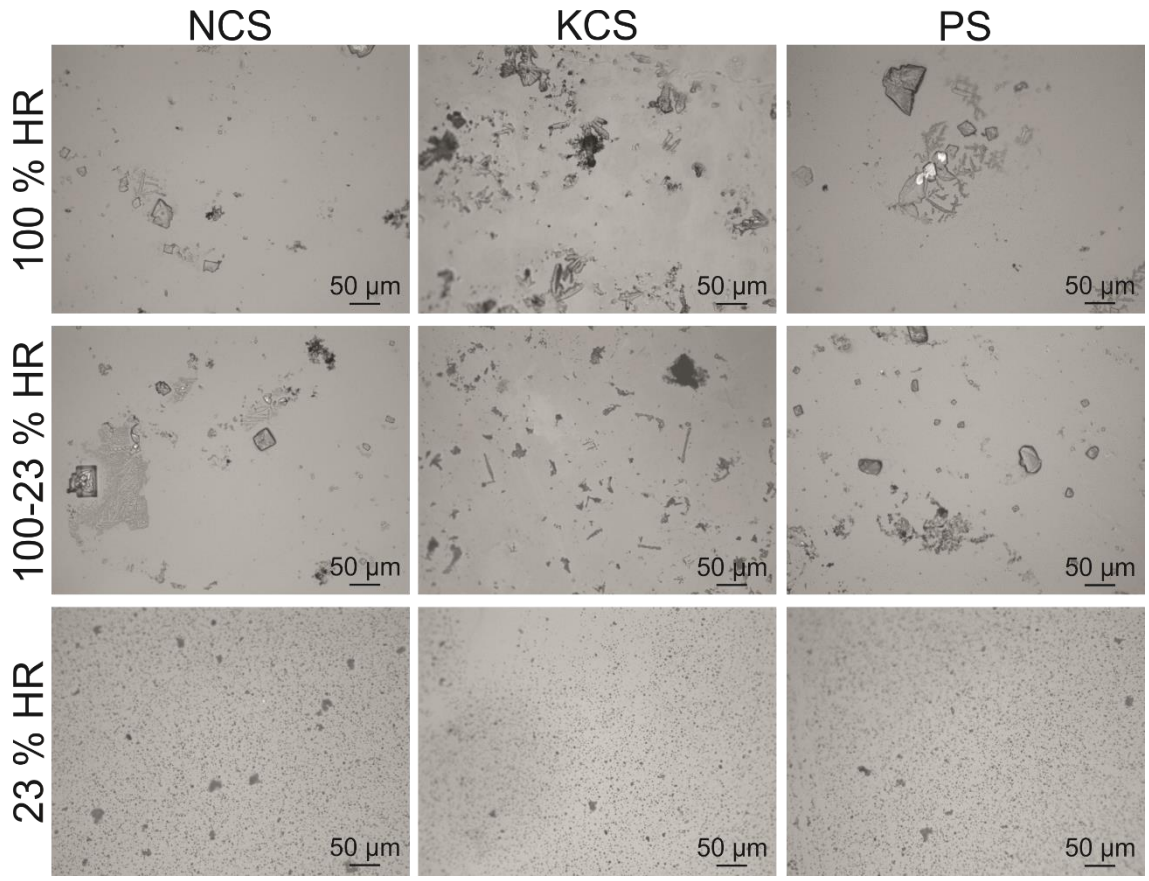

Fig. 2. OM images of the glass samples after 36 days of corrosion test.

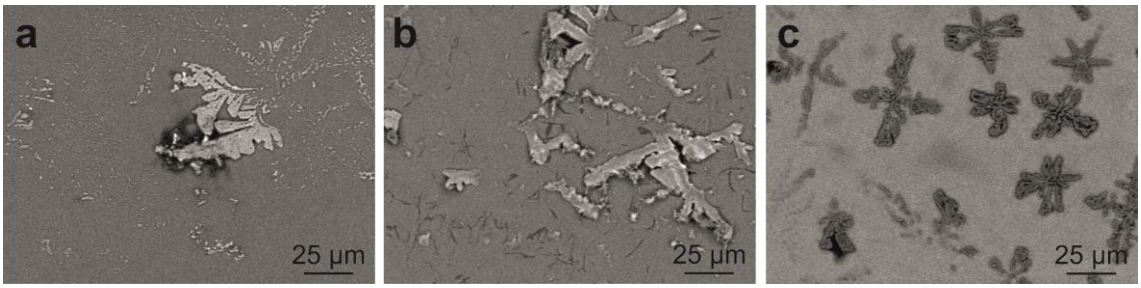

Fig. 3. SEM images of glass samples after 36 days at 100 % RH: a) NCS1, b) KCS1, c) PS1.

3.1.2. Composition of the deposits

GIXRD was carried out on the surface of the glass samples to identify the chemical composition of the deposits after the tests (Table 3). In general, those samples exposed to 100 % RH presented more complex species than on the other tests.

Soda-lime silicate glasses (NCS1, NCS2 and NCS3) only presented NaCl deposits (Table 3, Fig. 4) which were related with the original aerosols.

Potash-lime silicate glasses (KCS1, KCS2 and KCS3) presented NaCl deposits and also new crystalline phases on the surface of the glasses KCS1 and KCS2 (Table 3, Fig. 4). Not only chlorides were detected, also carbonates and sulfates were formed. High humidity favored the solubilization of atmospheric gases (CO_2 and SO_2) and the formation of complex species. These new species presented K^+ and Ca^{2+} ions which came from the ion exchange of the glass network with the Na^+ or H^+ ions from the surface water (Eq. 2, 3).

In lead silicate glasses (PS1, PS2 and PS3), the formation of new species (KCl, $PbCl_2$, PbOHCl and $CaCO_3$) was also favored (Table 3, Fig. 4). Similarly to previous glasses, high humidity favored the formation of complex species. Although, KCl and $PbCl_2$ were also identified in the samples exposed to 23 % RH (Table 3).

Table 3. Species identified by XRD in the surface of the glasses after 36 days of corrosion test.

Compound		NCS1	NCS2	NCS3	KCS1	KCS2	KCS3	PS1	PS2	PS3
Chlorides	Halite (NaCl)	✓	✓	✓	✓	✓	✓	✓	✓	✓
	Sylvite (KCl)				✓	✓		✓	✓	✓
	Cotunnite ($PbCl_2$)							✓		✓
	Lauronite (PbOHCl)							✓		
Carbonates	Natrite (Na_2CO_3)				✓					
	Calcite ($CaCO_3$)				✓	✓		✓		
Sulfates	Potassium sulfate (K_2SO_4)				✓	✓				

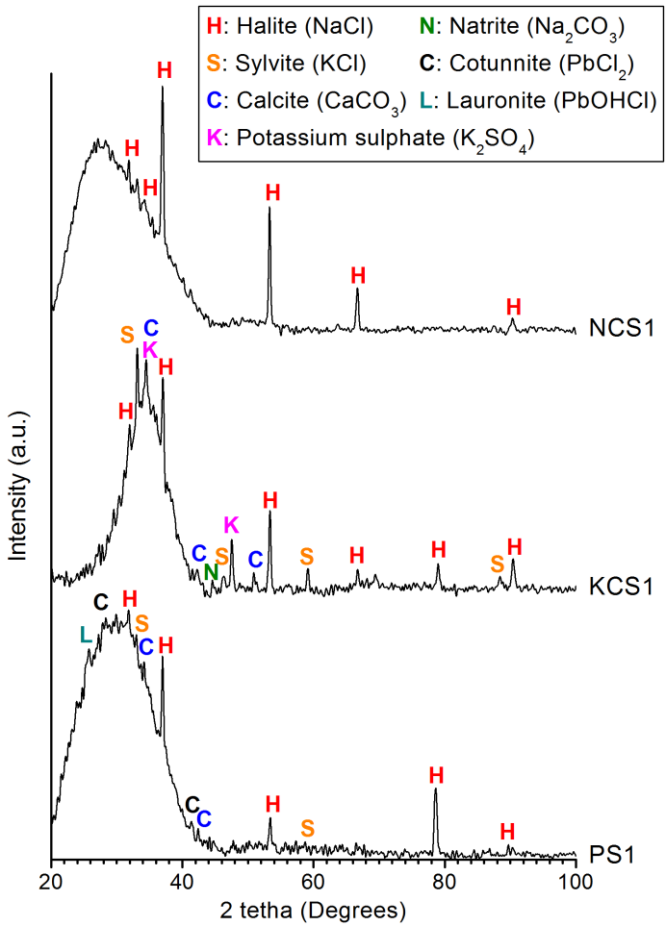

Fig. 4. XRD patterns of NCS1, KCS1 and PS1 after 36 days at 100 % RH.

3.1.3. Glass alteration

The alteration pathologies on the glass surface were identified by FTIR analyses. The samples exposed during 36 days at 100 % RH (NCS1, KCS1 and PS1) presented the stretching and bending of the hydroxyl groups (Fig. 5), in special in the sample KCS1. This stretching was related to the adsorption of molecular water in the glass surface and to the formation of hydroxyl groups due to the glass alteration [62].

Lead silicate glass was the less altered sample according to FTIR because their spectra before and after the exposition were very similar (Fig. 5). Soda-lime silicate glass presented a slight increase in the intensity of the symmetric stretching bands of SiO^- and the longitudinal optical (LO) component of the asymmetric stretching of SiO_2, which can be related to the formation of a very thin hydration layer on the glass surface. There was also observed a few increased in the stretching band of the carbonate ions (Fig. 5), even when they were not observed by XRD (Table 3, Fig. 4). In the case of potash-lime silicate glasses, the FTIR spectra showed a few increase in the asymmetric stretching bands of SiO_2, both the transverse optical (TO) and the longitudinal optical (LO) components (Fig. 5), which was related with the presence of a thin layer of hydrated silica on the glass surface [63]. Small fissures were observed previously by SEM (Fig. 3b). The stretching band of the carbonate experienced a high increase in the KCS glass after the lab corrosion test due to the formation of natrite (Na_2CO_3) and calcite ($CaCO_3$) on the glass surface (Figs. 4, 5, Table 3). The stretching band of the sulfate also experienced a few increase due to the formation of potassium sulfate (K_2SO_4) detected by XRD (Figs. 4, 5, Table 3).

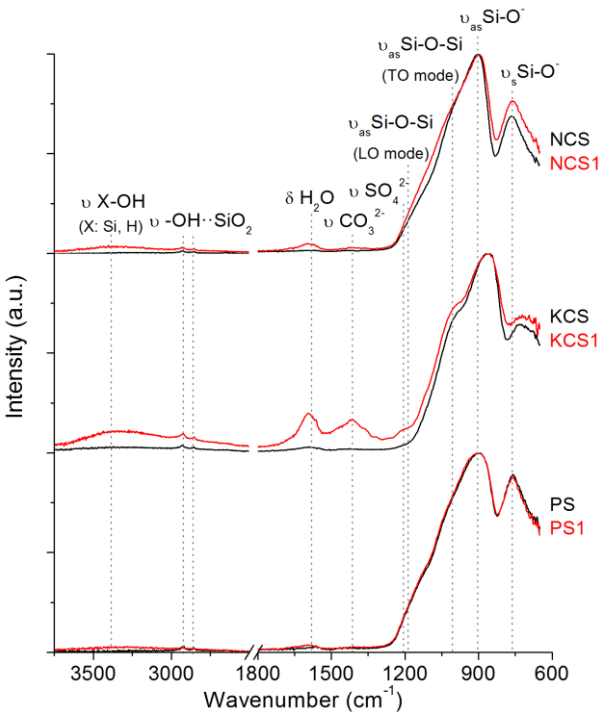

Fig. 5. Normalized FTIR spectra of the original samples (NCS, KCS and PS) and the samples after 36 days of corrosion test (NCS1, KCS1 and PS1). Types of vibrations: υ: stretching; δ: bending.

3.2. Cabo Vilano field exposure

3.2.1. Morphology of deposits

The surface of the samples exposed to the atmosphere in Cabo Vilano (Spain) was covered by small crystals (Figs. 6a, 6b, 6c). The soda-lime and potash-lime silicate glasses presented rectangle particles up to 3 μm of length and aggregations of small particles with an average diameter of 100 nm (Figs. 6a, 6b, 6d, 6e). This type of particles was also observed in the lead silicate glasses (Figs. 6c, 6f). The morphology of the salts was completely different to the CIME lab experiment (Figs. 3a, 3b , 3c) as aerosols were only pure NaCl with a concentration four times higher than in seawater [51], whereas in Cabo Vilano the aerosols were salts from the seawater and also soil particles from the environment. KCS was the only sample which presented fissures in the surface (Figs. 6b, 6e) which could be related with the formation of a surface alteration layer.

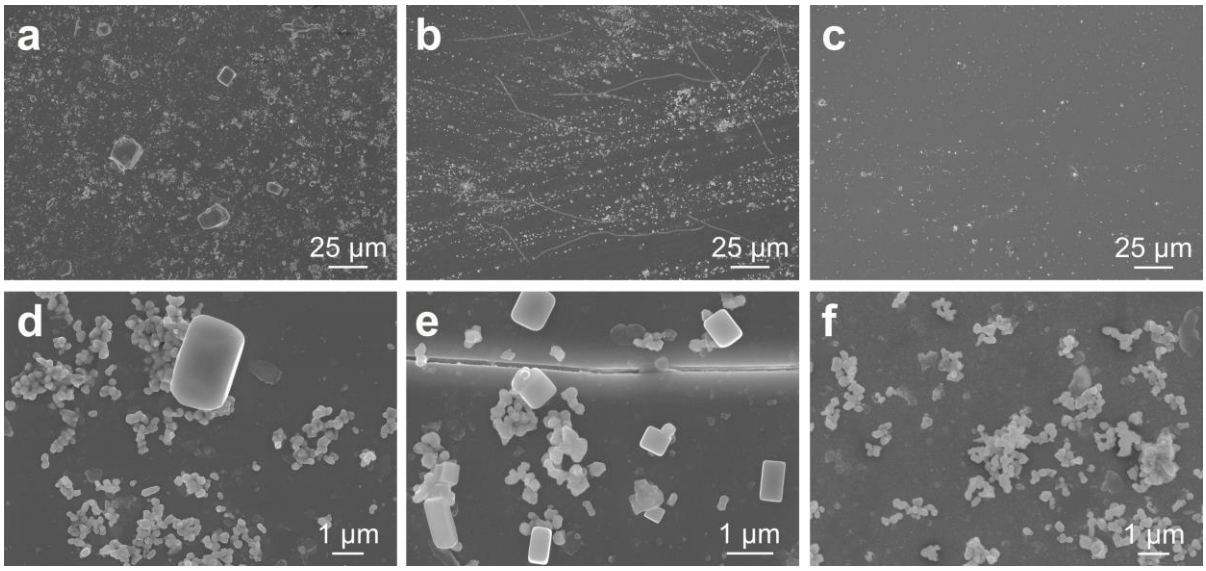

Fig. 6. SEM images of glass samples after the exposition in Cabo Vilano (Spain): a, d) NCS_CV; b, e) KCS_CV; c, f) PS_CV.

3.2.2. Composition of the deposits

The GIXRD analysis of the samples exposed in Cabo Vilano showed a high variety of crystals. All samples presented NaCl and KCl (Fig. 7), which can be associated with the composition of the seawater [51]. Calcite was detected in NCS_CV and KCS_CV, the glasses with higher contents of calcium (Table 1) and could come from the environment or can be formed during the alteration. The KCS_CV also presented natrite. In the lead silicate glass, lead chloride and lead carbonate were identified (Fig. 7) and they were related with the extraction of lead cations from the glass surface. Hematite (Fe_2O_3) and anatase (TiO_2) were also presented in all the samples.

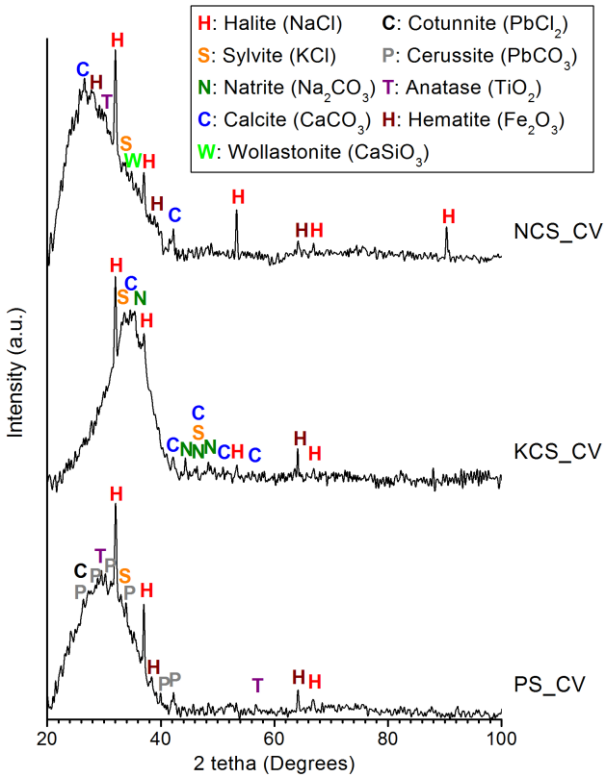

Fig. 7. XRD patterns of NCS_CV, KCS_CV and PS_CV after 36 days of exposure in Cabo Vilano (Spain).

The analysis of the particles with enough mass and active vibration modes can be detected by µ-Raman spectroscopy and showed the presence of rutile and red ochre particles (Fig. 8). These particles come from the environment. TiO_2 was detected by GIXRD in the crystalline form of anatase (Fig. 7). A phase transition could occur during the µ-Raman analysis transforming the anatase into rutile [64]. The red ochre, formed by a mixture of iron oxide, silica and clay, can be related with soil particles transported by wind.

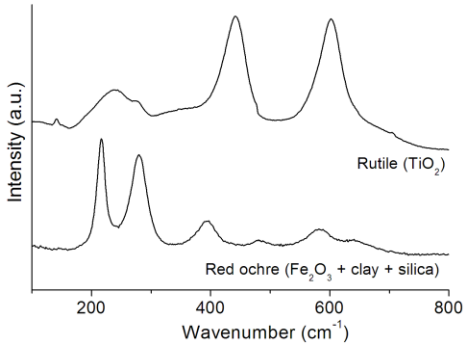

Fig. 8. µ-Raman spectra of particles on the samples exposed in Cabo Vilano (Spain).

3.2.3. Glass alteration

As result of the exposition in Cabo Vilano, all the samples presented the stretching and bending of the hydroxyl groups in the FTIR spectra due to the glass corrosion and the adsorption of water in the glass surface [62]. The stretching bands of carbonates or sulfates were not detected (Fig. 9).

Similarly to the lab corrosion test (section 3.1.3.), lead silicate and soda-lime silicate glass were the less altered samples because their spectra before and after the exposition were very similar (Fig. 9). Just a few increase in the intensity of the longitudinal optical (LO) component of the asymmetric stretching of SiO_2 and the symmetric stretching bands of SiO^- was detected in the soda-lime silicate glass spectrum, which was related to the formation of a hydration layer. On the contrary, the FTIR spectra of the potash-lime silicate glasses showed a completely different spectrum before and after the exposition due to the fast alteration of this type of glass. The asymmetric stretching bands of SiO_2, both the transverse optical (TO) and the longitudinal optical (LO) components, experienced a significant increase (Fig. 9), which was related with the presence of a porous silica layer on the glass surface [63]. The increase of these bands followed by the relative decrease of the asymmetric stretching band of $Si\text{-}O^-$ pointed to the formation of a surface alteration layer due to the dealkalization of the glass network (Eq. 2) followed by a condensation reaction (Eq. 1) [65, 66]. The formation of an alteration layer justified the significant increase of the stretching bands of the hydroxyl groups due to the adsorption of molecular water. Fissures in the alteration layer were previously observed by SEM (Figs. 6b, 6e).

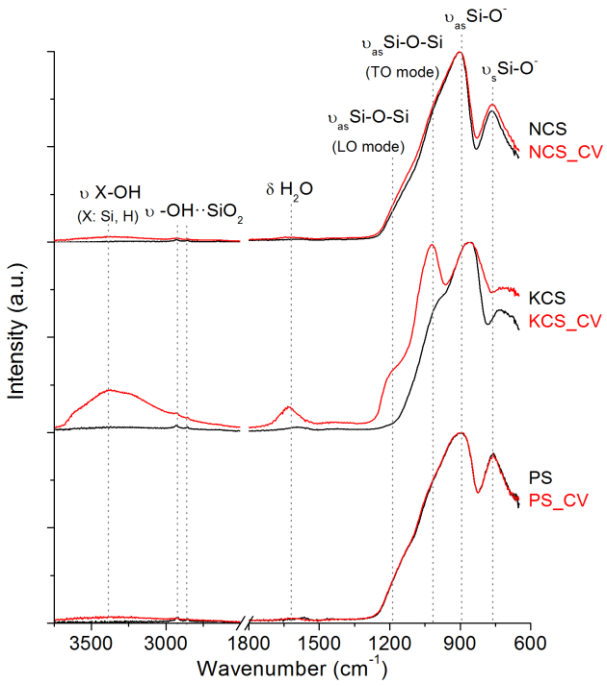

Fig. 9. Normalized FTIR spectra of the samples NCS, KCS and PS before and after the exposition in Cabo Vilano (Spain). Types of vibrations: υ: stretching; δ: bending.

The surface roughness of the glass was also modified during the exposition (Fig. 10). The original glass presented an almost flat surface due to the polishing in optical quality, just two micrometrical holes were detected (Fig. 10a). After exposure, all samples experienced an increase of the roughness (Figs. 10b, 10c, 10d), although the deposits on the surface were not observed due to their small size. The roughness of NCS sample was twice the original value, whereas KCS and PS presented an increase of approximately a factor 5 (Fig. 10).

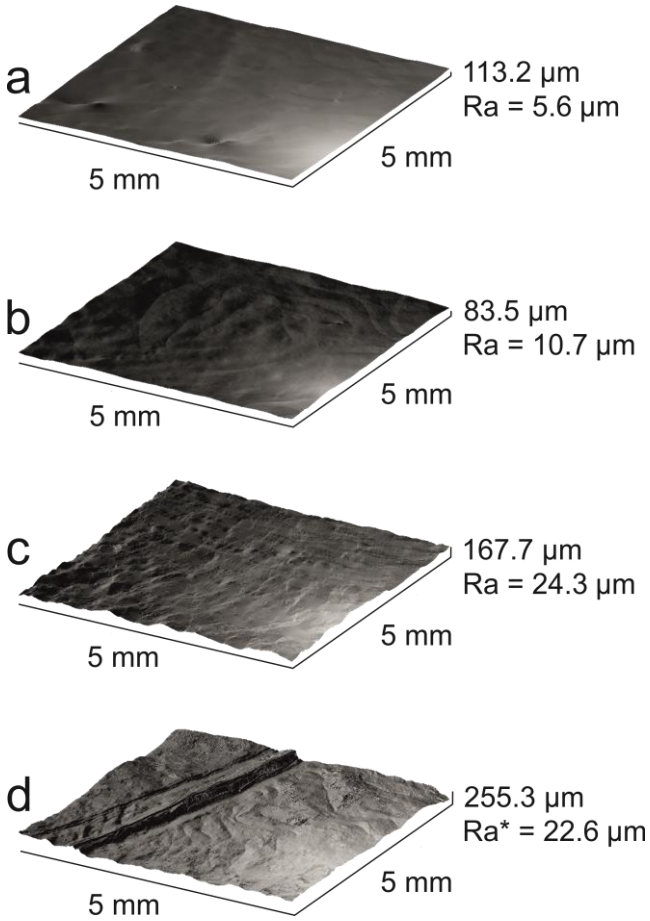

Fig. 10. Roughness maps from the surface of the samples a) NCS without be exposed, and the samples b) NCS_CV, c) KCS_CV, d) PS_CV after 36 days exposed in Cabo Vilano (Spain). The Z axis (µm) is the maximum value on the height and Ra is the arithmetic average roughness value determined by rugosimetry (5 × 5 mm) [58]. * The roughness was measured in a 2 × 2 mm area out of the cracks.

4. DISCUSSION

4.1. Effect of marine aerosols on the glass alteration

The results confirmed that high humidity favored the alteration of the glass surface and the formation of new crystalline phases. NaCl aerosols on the glass surface acted as condensation nuclei when the environmental relative humidity was above 76 % RH [59, 67]. The formation of a layer of water on the glass surface favored the lixiviation of the alkaline and alkaline-earth ions (Eqs. 2, 3) and the solubilization of atmospheric gases (CO_2, SO_2). During the CIME lab corrosion test a great diversity of crystalline phases were formed on the glasses which depended on the time and the

relative humidity. High humidity during long time favored the formation of complex species. Potash-lime silicate glasses exposed to the cycles 23/100 % RH also presented complex species due to the low stability of the glass composition. However in soda-lime silicate and lead silicate glasses, more stable compositions, the samples exposed to the cycles 23/100 % RH presented crystalline phases similar to the samples exposed to 23 % RH.

The formation of complex species was directly related to the Gibbs free energy of the salt and their solubility (Table 4). According to the Gibbs free energy, the evolution of the crystalline phases with sodium, potassium and calcium ions is: NaCl < KCl < $CaCl_2$ < Na_2CO_3 < $CaCO_3$ < K_2CO_3 < Na_2SO_4 < $CaSO_4$ < K_2SO_4 (Table 4). $CaCl_2$ and K_2CO_3 are intermediate species, but they were not detected in the corrosion tests because of their high solubility (Table 4). Na_2SO_4 and $CaSO_4$ were also not detected because they needed a high content of environmental SO_2 to be formed. This evolution was previously observed by Carmona et al. in historical medieval stained glass windows [22], where they showed that the carbonates acted as intermediate species in the formation of the corrosion crust of gypsum (Eq. 5, 6).

Table 4. Solubility at 25 ºC and Gibbs free energy of formation in standard conditions (25 ºC and 100 kPa) in aqueous solution of the species detected by XRD. Data obtained from [68], [69] [(a)] and [70][(b)].

Compound	Solubility $_{25\,^{\circ}C}$ (g/100 g H_2O)	ΔG_f° (kJ·mol^{-1})
NaCl	36	-393.1
Na_2CO_3	30.7	-1051.6
Na_2SO_4	28.1	-1268.4
KCl	35.5	-414.5
K_2CO_3	111	-1094.4
K_2SO_4	12	-1311.1
$CaCl_2$	81.3	-816.0
$CaCO_3$	$6.6\cdot10^{-4}$	-1081.4
$CaSO_4$	0.205	-1298.1
$PbCl_2$	1.08	-286.9
PbOHCl	-	- 383.7 [(a)]
$PbCO_3$	$1.1\cdot10^{-3}$ [(b)]	-625.9 [(b)]
$PbSO_4$	$4.3\cdot10^{-3}$ [(b)]	-813.9 [(b)]

In lead silicate glass, the formation of $PbCl_2$, PbOHCl, $PbCO_3$ and $PbSO_4$ was also thermodynamically favored (Table 4). Nevertheless, the Gibbs free energy of the species with lead was higher than the equivalent compounds with alkaline and alkaline-earth cations (Table 4), being the latter ones thermodynamically more stable. In addition, the lixiviation of the lead is less favored than the alkaline and alkaline-earth cations of potash-lime silicate glass, presenting comparatively a slow corrosion rate.

The salts detected in the samples exposed in Cabo Vilano (Spain) could be due to the deposition of marine aerosols and environmental particles, and also due to the reaction of the cations dissolved in the hydration water with the atmospheric CO_2 [22]. However, the diversity of new species was relatively poor because the rainwater washed the glass surface cleaning it.

4.2. Influence of glass composition on its alteration

Soda-lime silicate samples were the most stable glasses in both corrosion tests. The samples exposed to the CIME corrosion test only presented NaCl deposits on their surface which can be related to the original aerosols. The ion exchange could also occur on the glass surface, however the high concentration of Na^+ ions dissolved in the hydration water did not favor the dealkalization of ≡Si-O-Na. In the real environment, more variety of salts was detected on the glass surface. No alteration layer was observed on the glass, however a slight increase in both the hydroxyl bands in the FTIR spectra and the surface roughness were detected. This slight increase could be related with the hydration period in the alteration mechanism of the glass, which is the first step of the degradation of soda-lime silicate glasses in river and marine aqueous media [42]. Stable glasses, such as soda-lime silicates, present a slow and long hydration process in aqueous media [35], which could be even slower in atmospheric environments.

Lead silicate glass presented, in both tests, the formation of new crystalline species with lead, which just can proceed from the glass surface. The formation of these species demonstrates the ion exchange between the aerosols and the glass matrix. In addition, KCl was detected in the CIME lab corrosion test which proves that K^+ ions were also lixiviated. The surface, measured with the rugosimeter, was severely altered during the exposition to a real environment, however the FTIR spectra just showed a slightly increase in the band of the hydration layer. The FTIR bands between 1200 and 700 cm^{-1} are directly related with the bridging and non-bringing bonds in the silica network, which seems to be non-altered during the exposure. Previous studies have proven that lead silicate glasses are susceptible to atmospheric [71, 72] and marine environment [42, 73] because of the ion exchange between the H^+ ions of the medium and the Pb^{2+} cations in the glass network [74, 75]. Na^+ ions from NaCl aerosols could favor these reactions due to the opening of the network proposed in the alteration mechanism of the silica [35].

Finally, potash-lime silicate glass was the most altered glass in both corrosion tests. Humidity was the principal alteration agent because it favored the hydrolytic attack and lixiviation of the K^+ ions from the glass surface. This lixiviation left a very porous structure because the ionic radius of K^+ ions (R_{K+} = 0.133 nm) is higher than Na^+ and H^+ ions (R_{Na+} = 0.097 nm; R_{H+} = 0.010 m) [76]. This porous structure favored the diffusion of water molecules and Na^+ ions through the alteration layer. The FTIR bands related with the bridging bonds of the silica increased their intensity in relation with the non-bridging bonds. This relative increase was related to the polymerization of the silanol groups to form a porous silica layer [63]. In addition, the high tension of the structure formed several fissures in the alteration layer which were observed in both

experiments. The high concentration of Na^+ ions dissolved in the hydration layer could accelerate the alteration rate.

According to Dove and Crerar [35], the silanols groups formed during the hydrolytic attack can be replaced by ≡Si-O-Na groups which were placed perpendicularly to the surface to avoid the steric hindrance and the ionic repulsion favoring the opening the glass network. This substitution induced also the loss of the surface hydrogen bonds which protected the glass in acid medium favoring the alteration of the glass surface [4, 9, 12]. Regarding the crystals analyzed on the glass surface, complex salts formed by K^+ and Ca^{2+} cations lixiviated from the glass surface and environmental gases were detected in the CIME lab corrosion test. In the exposure on Cabo Vilano, the salts could be related with the glass alteration, such as in the CIME lab corrosion tests, and also due to aerosols.

5. CONCLUSIONS

Two tests were developed to determine the effect of marine aerosols on the alteration of silicate glasses. According to the results, NaCl aerosols have two main effects on the glass surface. The first one is that they acted as condensation nuclei in high humidity environments. The hydrated surface favored the lixiviation of alkaline and alkaline-earth ions from the surface and the solubilization of atmospheric gases (CO_2, SO_2). The salts detected after the tests presented a great diversity of crystalline phases.

According to the Gibbs free energies, the evolution of these compounds are chlorides < carbonates < sulfates, however not all the intermediate species were detected due to the solubility of each salt. The second effect is that the Na^+ ions dissolved in the hydration layer can accelerate the corrosion attack due to the

replacement of ≡Si-O-H groups by ≡Si-O-Na. This substitution induced the loss of the surface hydrogen bonds and the opening of the network accelerating the corrosion mechanism.

Regarding the type of glass, soda-lime silicate glass was the most durable one because of its high stability to environmental conditions. Lead silicate glass was not present any alteration pathology, however it experienced the lixiviation of Pb^{2+} ions to form lead chloride and lead carbonate. Finally, potash-lime silicate glass was the less durable glass because it presented a fissured alteration layer due to the hydrolytic attack of the surface. In addition, several compounds with K^{+} and Ca^{2+} ions were detected due to the dealkalization of the surface.

Moreover, this study highlights that airborne particles of natural origin such as marine aerosols have the ability to modify the properties of the glass surface and to favor its surface dealkalization in a very short exposure time (1 to 3 months only).

Acknowledgments

The authors thank to F. Agua and J.F. Conde (CCHS-CSIC, Spain) for the preparation of the glass samples, to E. Peiteado (ICV-CSIC, Spain) for the contact angle measurements, to A. Tomás (CENIM-CSIC, Spain) for his help during the SEM observations, to C. Vázquez-Calvo (IGEO-CSIC-UCM, Spain) for her assistance during the microroughness measurements, to Fedakar Movil S.L.L. (Tres Cantos, Spain) for painting the support structures, and to ENEL and Gas Natural for the facilities provided at Cabo Vilano wind farm for the setting up of corrosion stations and data collection. This work was initiated during a short stay financed by the Erasmus+ staff mobility program and has been partially funded by the Fundação do Ministério de Ciência e Tecnologia de Portugal (Project ref. UID/EAT/00729/2013 and Post-doctoral grant ref.

SFRH/BPD/108403/2015) and GEOMATERIALES 2-CM Program Ref. S2013/MIT-2914. Professional support from Techno-Heritage (Network on Science and Technology for the Conservation of Cultural Heritage) is also acknowledged.

REFERENCES

[1] T. Lombardo, A. Ionescu, R.A. Lefèvre, A. Chabas, P. Ausset, H. Cachier, Soiling of silica-soda-lime float glass in urban environment: measurements and modelling, Atmos. Environ., 39 (2005) 989-997.
[2] T. Lombardo, A. Chabas, A. Verney-Carron, H. Cachier, S. Triquet, S. Darchy, Physico-chemical characterisation of glass soiling in rural, urban and industrial environments, Environ. Sci. Pollut. R., 21 (2014) 9251-9258.
[3] T.M. El-Shamy, Chemical durability of K_2O-CaO-MgO-SiO_2 glasses, Phys. Chem. Glasses, 14 (1973) 1-5.
[4] R.H. Doremus, Infrared spectroscopy of surfaces of glasses containing alkali ions, J. Non-Cryst. Solids, 41 (1980) 145-149.
[5] M. Schreiner, G. Woisetschläger, I. Schmitz, M. Wadsak, Characterisation of surface layers formed under natural environmental conditions on medieval stained glass and ancient copper alloys using SEM, SIMS and atomic force microscopy, J. Anal. At. Spectrom., 14 (1999) 395-403.
[6] M. De Bardi, H. Hutter, M. Schreiner, ToF-SIMS analysis for leaching studies of potash–lime–silica glass, Appl. Surf. Sci., 282 (2013) 195-201.
[7] K. Cummings, W.A. Lanford, M. Feldmann, Weathering of glass in moist and polluted air, Nucl. Instrum. Meth. B, 136-138 (1998) 858-862.
[8] T.M. El-Shamy, S.E. Morsi, H.D. Taki-Eldin, A.A. Ahmed, Chemical durability of Na_2O-CaO-SiO_2 glasses in acid solutions, J. Non-Cryst. Solids, 19 (1975) 241-250.
[9] W.A. Lanford, K. Davis, P. Lamarche, T. Laursen, R. Groleau, R.H. Doremus, Hydration of soda-lime glass, J. Non-Cryst. Solids, 33 (1979) 249-266.
[10] B.C. Bunker, Molecular mechanisms for corrosion of silica and silicate glasses, J. Non-Cryst. Solids, 179 (1994) 300-308.
[11] T. Lombardo, L. Gentaz, A. Verney-Carron, A. Chabas, C. Loisel, D. Neff, E. Leroy, Characterisation of complex alteration layers in medieval glasses, Corros. Sci., 72 (2013) 10-19.
[12] T.M. El-Shamy, J. Lewins, R.W. Douglas, The dependence on the pH of the decomposition of glasses by aqueous solutions, Glass Technol., 13 (1972) 81-87.
[13] E. Greiner-Wronowa, L. Stoch, Influence of environment on surface of the ancient glasses, J. Non-Cryst. Solids, 196 (1996) 118-127.
[14] T. Lombardo, C. Loisel, L. Gentaz, A. Chabas, M. Verita, I. Pallot-Frossard, Long term assessment of atmospheric decay of stained glass windows, Corros. Eng. Sci. Techn., 45 (2010) 420-424.
[15] T. Palomar, La interacción de los vidrios históricos con medios atmosféricos, acuáticos y enterramientos. PhD dissertation, Universidad Aunónoma de Madrid (Spain), 2013.
[16] M. Pérez-y-Jorba, J. Dallas, R. Collongues, C. Bahezre, J. Martin, Étude del'alteration des vitraux anciens par microscopie electronique a balayage et microsonde, Silic. Ind., 43 (1978) 89-99.
[17] K. Bange, O. Anderson, F. Rauch, P. Lehuede, E. Rädlein, N. Tadokoro, P. Mazzoldi, V. Rigato, K. Matsumoto, M. Farnworth, Multi-method characterization of soda-lime glass corrosion. Part 2. Corrosion in humidity, Glass Sci. Technol., 75 (2002) 20-33.

[18] L. Gentaz, T. Lombardo, A. Chabas, C. Loisel, A. Verney-Carron, Impact of neocrystallisations on the SiO_2–K_2O–CaO glass degradation due to atmospheric dry depositions, Atmos. Environ., 55 (2012) 459-466.
[19] L. Gentaz, T. Lombardo, A. Chabas, C. Loisel, D. Neff, A. Verney-Carron, Role of secondary phases in the scaling of stained glass windows exposed to rain, Corros. Sci., 109 (2016) 206-216.
[20] G. WoisetschlaÈger, M. Dutz, S. Paul, M. Schreiner, Weathering phenomena on naturally weathered potash-lime-silica-glass with medieval composition studied by secondary electron microscopy and energy dispersive microanalysis, Mikrochim. Acta, 135 (2000) 121-130.
[21] M. Garcia-Vallès, D. Gimeno-Torrente, S. Martínez-Manent, J.L. Fernández-Turiel, Medieval stained glass in a Mediterranean climate: Typology, weathering and glass decay, and associated biomineralization processes and products, Am. Mineral., 88 (2003) 1996-2006.
[22] N. Carmona, M.A. Villegas, J.M.F. Navarro, Characterisation of an intermediate decay phenomenon of historical glasses, J. Mater. Sci., 41 (2006) 2339-2346.
[23] M. Aulinas, M. Garcia-Valles, D. Gimeno, J.L. Fernandez-Turiel, F. Ruggieri, M. Pugès, Weathering patinas on the medieval (s. XIV) stained glass windows of the Pedralbes Monastery (Barcelona, Spain), Environ. Sci. Pollut. R., 16 (2008) 443.
[24] M. Vilarigues, P. Redol, A. Machado, P.A. Rodrigues, L.C. Alves, R.C. da Silva, Corrosion of 15^{th} and early 16^{th} century stained glass from the monastery of Batalha studied with external ion beam, Mater. Charact., 62 (2011) 211-217.
[25] M. García-Heras, C. Gil, N. Carmona, M.A. Villegas, Efectos de la meteorización sobre los materiales de las vidrieras históricas, Mater. Construcc., 53 (2003) 21-34.
[26] M. Vilarigues, R.C. da Silva, Ion beam and infrared analysis of medieval stained glass, Appl. Phys. A, 79 (2004) 373-378.
[27] L. Gentaz, T. Lombardo, C. Loisel, A. Chabas, M. Vallotto, Early stage of weathering of medieval-like potash–lime model glass: evaluation of key factors, Environ. Sci. Pollut. R., 18 (2011) 291-300.
[28] J. Hormes, A. Roy, G.L. Bovenkamp, K. Simon, C.Y. Kim, N. Börste, S. Gai, Medieval glass from the Cathedral in Paderborn: a comparative study using X-ray absorption spectroscopy, X-ray fluorescence, and inductively coupled laser ablation mass spectrometry, Appl. Phys. A, 111 (2013) 91-97.
[29] H.V. Walters, P.B. Adams, Effects of humidity on the weathering of glass, J. Non-Cryst. Solids, 19 (1975) 183-199.
[30] N. Carmona, M.A. Villegas, J.M. Fernández Navarro, Corrosion behaviour of R_2O–CaO–SiO_2 glasses submitted to accelerated weathering, J. Eur. Ceram. Soc., 25 (2005) 903-910.
[31] M. Melcher, M. Schreiner, K. Kreislova, Artificial weathering of model glasses with medieval compositions– an empirical study on the influence of particulates, Phys. Chem. Glasses, 49 (2008) 346-356.
[32] K. Torfs, R. Van Grieken, Chemical relations between atmospheric aerosols, deposition and stone decay layers on historic buildings at the mediterranean coast, Atmos. Environ., 31 (1997) 2179-2192.
[33] C. Cardell, F. Delalieux, K. Roumpopoulos, A. Moropoulou, F. Auger, R. Van Grieken, Salt-induced decay in calcareous stone monuments and buildings in a marine environment in SW France, Constr. Build. Mater., 17 (2003) 165-179.
[34] N.-A. Stefanis, P. Theoulakis, C. Pilinis, Dry deposition effect of marine aerosol to the building stone of the medieval city of Rhodes, Greece, Build. Environ., 44 (2009) 260-270.
[35] P.M. Dove, D.A. Crerar, Kinetics of quartz dissolution in electrolyte solutions using a hydrothermal mixed flow reactor, Geochim. Cosmochim. Ac., 54 (1990) 955-969.
[36] P.M. Dove, S.F. Elston, Dissolution kinetics of quartz in sodium chloride solutions: Analysis of existing data and a rate model for 25°C, Geochim. Cosmochim. Ac., 56 (1992) 4147-4156.
[37] H. Strandh, L. Sjöberg, L.G.M. Pettersson, U. Wahlgren, A theoretical and experimental study of quartz dissolution dependence on alkali metal cations, GFF, 118 (1996) 55-56.

[38] P.M. Dove, C.J. Nix, The influence of the alkaline earth cations, magnesium, calcium, and barium on the dissolution kinetics of quartz, Geochim. Cosmochim. Ac., 61 (1997) 3329-3340.
[39] P.M. Dove, The dissolution kinetics of quartz in aqueous mixed cation solutions, Geochim. Cosmochim. Ac., 63 (1999) 3715-3727.
[40] J.P. Icenhower, P.M. Dove, The dissolution kinetics of amorphous silica into sodium chloride solutions: effects of temperature and ionic strength, Geochim. Cosmochim. Ac., 64 (2000) 4193-4203.
[41] C.L. Wickert, A.E. Vieira, J.A. Dehne, X. Wang, D.M. Wilder, A. Barkatt, Effects of salts on silicate glass dissolution in water: kinetics and mechanisms of dissolution and surface cracking, Phys. Chem. Glasses, 40 (1999) 157-170.
[42] T. Palomar, I. Llorente, Decay processes of silicate glasses in river and marine aquatic environments, J. Non-Cryst. Solids, 449 (2016) 20-28.
[43] M. Melcher, M. Schreiner, Evaluation procedure for leaching studies on naturally weathered potash-lime-silica glasses with medieval composition by scanning electron microscopy, J. Non-Cryst. Solids, 351 (2005) 1210-1225.
[44] M. Melcher, M. Schreiner, Leaching studies on naturally weathered potash-lime–silica glasses, J. Non-Cryst. Solids, 352 (2006) 368-379.
[45] M. Kottek, J. Grieser, C. Beck, B. Rudolf, F. Rubel, World Map of the Köppen-Geiger climate classification updated, World Map of the Köppen-Geiger climate classification updated, 15 (2006) 259-263.
[46] R.E. Smallman, R.J. Bishop, Modern physical metallurgy and materials engineering: Science, process, applications. 6th edition, Butterworth-Heinemann, Oxford, 1999.
[47] J.-M. Bettembourg, Composition et altération des verres de vitraux anciens, in: Verres et réfractaires. Actes du IX colloque international du Corpus Vitrearum Medii Aevi, Paris, 8-12 September 1975, 1976, pp. 36-42.
[48] N. Carmona, M. Oujja, E. Rebollar, H. Römich, M. Castillejo, Analysis of corroded glasses by laser induced breakdown spectroscopy, Spectrochim. Acta B, 60 (2005) 1155-1162.
[49] UNE 43603, Vidrio. Nomenclatura y terminología. Cristal. Vidrio Sonoro, 1979.
[50] A. Chabas, A. Fouqueau, M. Attoui, S.C. Alfaro, A. Petitmangin, A. Bouilloux, M. Saheb, A. Coman, T. Lombardo, N. Grand, P. Zapf, R. Berardo, M. Duranton, R. Durand-Jolibois, M. Jerome, E. Pangui, J.J. Correia, I. Guillot, S. Nowak, Characterisation of CIME, an experimental chamber for simulating interactions between materials of the cultural heritage and the environment, Environ. Sci. Pollut. R., 22 (2015) 19170-19183.
[51] F.J. Millero, Chemical oceanography, CRC press, Taylor & Francis Group, Boca Raton, 2006.
[52] D.C. Blanchard, A.H. Woodcock, The production, concentration, and vertical distribution of the sea-salt aerosol, Ann. NY Acad. Sci., 338 (1980) 330-347.
[53] P. Buxton, K. Mellanby, The measurement and control of humidity, B. Entomol. Res., 25 (1934) 171-175.
[54] L. Greenspan, Humidity fixed points of binary saturated aqueous solutions, J. Res. Nat. Bur. Stand., 81A (1977) 89-96.
[55] UNE-EN ISO 9225:2012, Corrosión de los metales y aleaciones. Corrosividad de atmósferas. Medida de los parámetros ambientales que afectan a la corrosividad de las atmósferas, 2012.
[56] M. Morcillo, B. Chico, J. Alcántara, I. Díaz, J. Simancas, D. de la Fuente, Atmospheric corrosion of mild steel in chloride-rich environments. Questions to be answered, Mater. Corros., 66 (2015) 882-892.
[57] V. Thomsen, Basic fundamental parameters in X-ray fluorescence, Spectroscopy, 22 (2007) 46-50.
[58] DIN EN ISO 4287, Surface roughness - terminology: Part 1. Surface and its parameters, 1998.

[59] M.E. Wise, T.A. Semeniuk, R. Bruintjes, S.T. Martin, L.M. Russell, P.R. Buseck, Hygroscopic behavior of NaCl-bearing natural aerosol particles using environmental transmission electron microscopy, J. Geophys. Res.-Atmos., 112 (2007) 1-10.
[60] Y. Yuan, T.R. Lee, Contact angle and wetting properties, in: G. Bracco, B. Holst (Eds.) Surface Science Techniques, Springer Berlin Heidelberg, Berlin, Heidelberg, 2013, pp. 3-34.
[61] R. Bahadur, L.M. Russell, Water uptake coefficients and deliquescence of NaCl nanoparticles at atmospheric relative humidities from molecular dynamics simulations, J. Chem. Phys., 129 (2008) 094508.
[62] R.F. Bartholomew, B.L. Butler, H.L. Hoover, C.K. Wu, Infrared spectra of a water-containing glass, J. Am. Ceram. Soc., 63 (1980) 481-485.
[63] R.M. Almeida, C.G. Pantano, Structural investigation of silica gel films by infrared spectroscopy, J. Appl. Phys., 68 (1990) 4225-4232.
[64] P.C. Ricci, C.M. Carbonaro, L. Stagi, M. Salis, A. Casu, S. Enzo, F. Delogu, Anatase-to-rutile phase transition in TiO_2 nanoparticles irradiated by visible light, J. Phys. Chem. C, 117 (2013) 7850-7857.
[65] M. Vilarigues, R.C. da Silva, Characterization of potash-glass corrosion in aqueous solution by ion beam and IR spectroscopy, J. Non-Cryst. Solids, 352 (2006) 5368-5375.
[66] M.E. Lynch, D.C. Folz, D.E. Clark, Use of FTIR reflectance spectroscopy to monitor corrosion mechanisms on glass surfaces, J. Non-Cryst. Solids, 353 (2007) 2667-2674.
[67] I.N. Tang, H.R. Munkelwitz, Aerosol phase transformation and growth in the atmosphere, J. Appl. Meteorol., 33 (1994) 791-796.
[68] CRC Handbook of chemistry and physics, Internet version 2005, CRC Press, Boca Raton, Florida. URL: http://www.hbcpnetbase.com, 2005.
[69] D.A. Humphreys, J.H. Thomas, P.A. Williams, R.F. Symes, The chemical stability of mendipite, diaboléite, chloroxiphite, and cumengéite, and their relationships to other secondary lead (II) minerals, Mineral. Mag., 43 (1980) 901-904.
[70] P. Patnaik, Handbook of inorganic chemicals, McGraw-Hill, New York, 2003.
[71] M. Schreiner, G. Stingeder, M. Grasserbauer, Quantitative characterization of surface layers on corroded medieval window glass with SIMS, Fresen. Z. Anal. Chem., 319 (1984) 600-605.
[72] C.S. Salerno, C. Moretti, T. Medici, T. Morna, M. Verità, Glass weathering in eighteenth century mosaics: The São João Chapel in the São Roque Church in Lisbon, J. Cult. Herit., 9, Supplement (2008) e37-e40.
[73] N. Carmona, M. García-Heras, C. Gil, M.A. Villegas, Chemical degradation of glasses under simulated marine medium, Mater. Chem. Phys., 94 (2005) 92-102.
[74] C. Schultz-Münzenberg, W. Meisel, P. Gütlich, Changes of lead silicate glasses induced by leaching, J. Non-Cryst. Solids, 238 (1998) 83-90.
[75] F.H. El-Batal, E.M.A. Khalil, Y.M. Hamdy, H.M. Zidan, M.S. Aziz, A.M. Abdelghany, Infrared reflection spectroscopy for precise tracking of corrosion behavior in 3d-transition metals doped binary lead silicate glass, Physica B, 405 (2010) 2648-2653.
[76] F. Burriel Martí, F. Lucena Conde, S. Arribas Jimeno, J. Hernández Méndez, Química analítica cualitativa, 18th edition, Thomson, Madrid, 2002.